

## Research Article

**Comparative Synthetic Study, *in silico* Screening and Biological Evaluation of some Substituted Tetrahydropyrimidine-2-thione Derivatives as Potential DHFR Inhibitors****M. S. Bhosale<sup>1\*</sup>, K. Saravanan<sup>2</sup>**<sup>1</sup>Department of Pharmaceutical Chemistry, Bhagwant University, Ajmer.\*Corresponding Author Email: [mayurbhosale2399@gmail.com](mailto:mayurbhosale2399@gmail.com)

---

*Received: 15 Nov 2021;**Revised: 05 Dec 2021;**Accepted and Published: 19 Dec 2021*

---

**Abstract**

In present study we have selected pyrimidine scaffold to design and develop some DHFR inhibitors as potential antibacterial and antifungal agents. The designed derivatives were first screened through ADMET property calculations and then those possess drug-likeness properties were subjected for the molecular docking studies. The derivatives which were found to be significant DHFR inhibition potential were subjected for the synthesis followed by spectral analysis and biological evaluation. From this virtual screening, it was concluded that all the compounds possess drug-like properties and hence were subjected to molecular docking studies. The selected derivatives were synthesized and subjected for *in vitro* biological evaluation. The comparative study for synthesis of the derivatives such as conventional, ultrasonic, microwave synthesis was carried out. It was also observed that yield of the compound was very good in microwave assisted synthesis i.e. 80.50% which is almost 30-40% more than that of the conventional and ultrasonic method. In mass spectrum it was observed that, product obtained through microwave method was completely pure and did not displayed any peak of starting material, whereas product obtained through conventional and ultrasonic method showed presence of starting material. Therefore we concluded that the microwave assisted synthesis method is most suitable for the synthesis of tetrahydropyrimidine-2-thione derivatives through Biginelli reaction. We hereby report that, all the compounds **B1, B2, B3, B4, B5, B6, B7** and **B8** were found to be are potent and can be developed further to get more promising molecules for the treatment of bacterial & fungal infections.

**Keywords:** DHFR; tetrahydropyrimidine; Biginelli reaction; antibacterial activity, microwave

## Introduction

The advent of germs resistant to the majority of commonly used treatment drugs is one of the most severe threats to public health today(1,2). Drug-resistant bacteria like methicillin-resistant *Staphylococcus aureus* (MRSA) and multidrug-resistant *Escherichia coli* make treating nosocomial infections very challenging, posing a serious danger to global public health.(3–5). According to a UK Government analysis, "the cost in terms of lost global productivity between now and 2050 will be an astonishing 100 trillion USD if we do not take action". Fungal infections can represent a major hazard to human health, particularly in immunocompromised people.

Inhibitors of dihydrofolate reductase (DHFR), an important enzyme in the folate biosynthesis pathway, have been explored for many decades as therapies in the treatment of human malignancies. DHFR catalyzes the transfer of a hydride from the cofactor, nicotinamide adenine dinucleotide phosphate (NADPH), to the substrate, dihydrofolate, thereby generating tetrahydrofolate and NADP<sup>+</sup>. Tetrahydrofolate is an important cofactor in the formation of purines and thymidylate and its shortage leads to the suppression of cell development and proliferation.(6–9).

Compounds based on the pyrimidine scaffold are known to exhibit many different biological actions such as antibacterial, antifungal, anti-inflammatory and antitumor activities(10–12). Lots of amino pyrimidine-based derivatives have been reported to exhibit antibacterial activities via inhibiting DHFR(13,14). Therefore, in present study we have selected pyrimidine scaffold to design and develop some DHFR inhibitors as potential antibacterial and antifungal agents. The designed derivatives were first screened through ADMET property calculations and then those possess drug-likeness properties were subjected for molecular docking studies. The derivatives which were found to be significant DHFR inhibition potential were subjected for synthesis followed spectral analysis and biological evaluation. The comparative study for synthesis of the derivatives such as conventional, ultrasonic, and microwave synthesis was carried out. The one compound synthesized from each method were studied to prove the most effective method.

## Materials and methods

### Pharmacokinetics and toxicity predictions of designed derivatives

Utilizing molinspiration and SwissADME servers, Lipinski rule of five and pharmacokinetic features of developed derivatives were investigated(15,16). An *in silico* toxicity prediction of designed derivatives has been made using ProTox-II, a webserver that is freely available([http://tox.charite.de/protox\\_II](http://tox.charite.de/protox_II))(17).

### Molecular Docking

After screening through *in silico* ADMET analysis, the screened molecules were subjected for the molecular docking studies. The proposed derivatives and the native ligand were docked against the crystal structure of the wild-type *E. coli* dihydrofolate reductase using Autodockvina 1.1.2 in PyRx 0.8(18). ChemDraw Ultra 8.0 was used to draw the structures of the intended derivatives and native ligand (mole. File format). All the ligands were subjected for energy minimization by applying Universal Force Field (UFF)(19). RCSB Protein Data Bank (PDB) entry 5CCC contains the wild-type *E. coli* dihydrofolate reductase complexed with 5,10-dideazatetrahydrofolate and oxidized nicotinamide adenine dinucleotide phosphate (<https://www.rcsb.org/structure/5CCC>). Discovery Studio Visualizer (version-19.1.0.18287) was used to refine the enzyme structure, purify it, and get it ready for docking(20). A three-dimensional grid box (size\_x=30.6812046484Å; size\_y=32.6755842638Å; size\_z=35.0196745629Å) with an exhaustiveness value of 8 was created for molecular docking(18). BIOVIA Discovery Studio Visualizer was used to locate the protein's active amino acid residues. The approach outlined by Khan et al. was used to perform the entire molecular docking procedure, identify cavity and active amino acid residues(21–25). Fig. 1 shows the revealed cavity of DHFR with the co-crystallize ligand molecule.

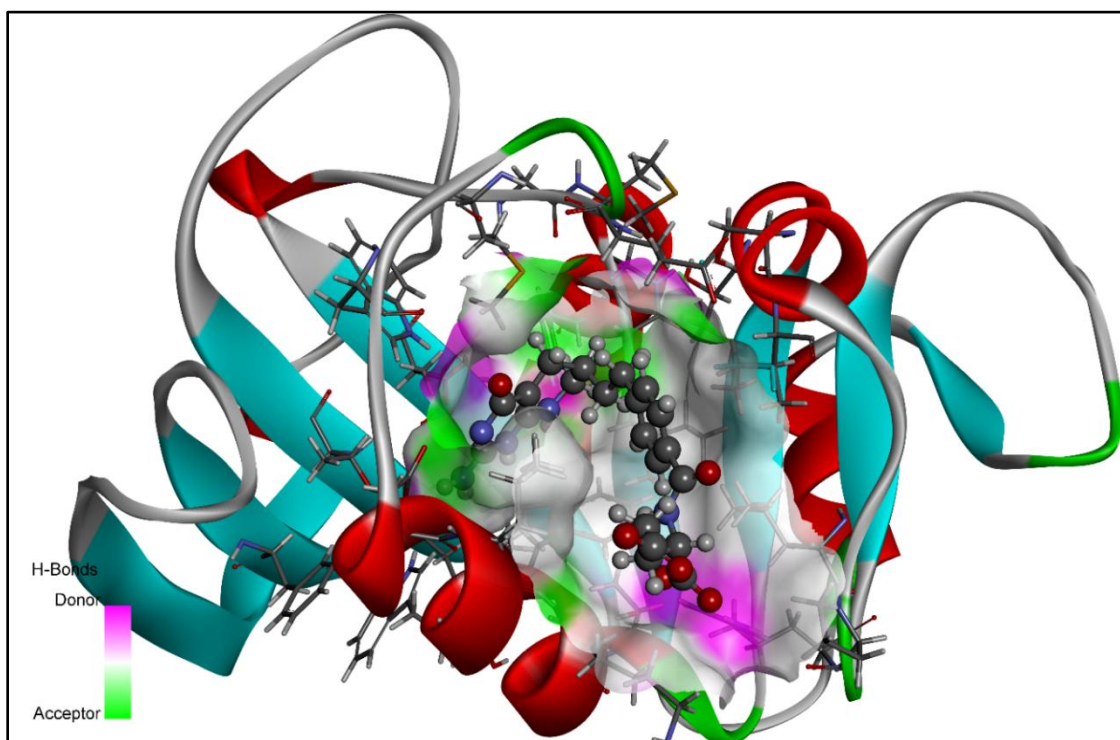


**Fig.1.** 3D ribbon view of DHFR with native ligand in allosteric site

### Reaction Scheme and Synthesis of derivatives

All the required chemicals i.e. ethyl acetoacetate, aldehyde, urea, ferric chloride ( $\text{FeCl}_3 \cdot 6\text{H}_2\text{O}$ ), conc. HCl, ethanol, potassium hydroxide (KOH), and acetone of synthetic grade were purchased and procured from Lab Trading Laboratory, Aurangabad, Maharashtra, India. The progress of the reaction was confirmed by Thin-layer chromatography [TLC, (Merck precoated silica GF 254)] and compounds were subjected for spectral analysis by  $^1\text{H}$ ,  $^{13}\text{C}$  NMR (on a Varian-VXR-300S at 400 MHz NMR spectrometer) and Mass spectroscopy with chloroform ( $d_6$ ) as the solvent and TMS as the internal standard; chemical shift values were expressed in  $\delta$  ppm. The melting points were measured using the VEEGO MODEL VMP-D melting point apparatus. The detailed procedure for the synthesis of derivatives is discussed in the below section.

### Synthesis of 1,2,3,4-tetrahydropyrimidine derivatives

#### 1) Conventional synthesis

The reaction is a modified Biginelli reaction that generates 1,2,3,4-tetrahydropyrimidine-2- one from ethyl acetoacetate, aldehyde and thiourea. A solution of ethyl acetoacetate (1.3gm, 10 mmol), urea (1.14gm, 15 mmol), ferric chloride ( $\text{FeCl}_3 \cdot 6\text{H}_2\text{O}$ , 2.5 mmol) and conc. HCl (1-2

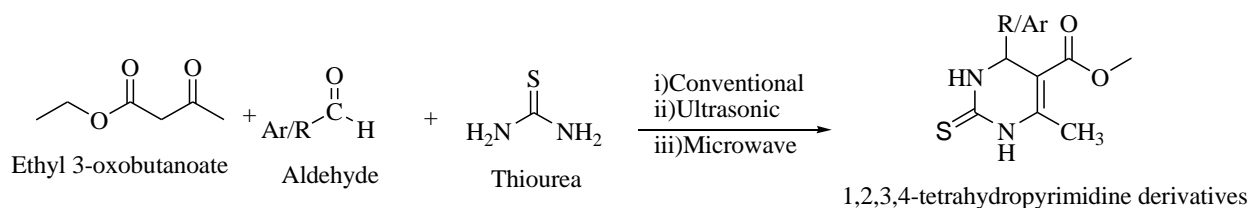
drops) in EtOH (20 mL) was heated independently with appropriate aldehydes (10 mmol), under reflux for 4-5 hrs(26). After cooling, the reaction mixtures were poured onto crushed ice (100gm). Stirring was continued for several minutes, the solid products were filtered, independently washed with cold H<sub>2</sub>O (2 times 50 mL) and a mixture of EtOH-H<sub>2</sub>O, 1:1 (3 times 20 mL). The solids were dried and recrystallized from hot EtOH to afford pure products. The melting point was recorded. The yields obtained were in the range of 75-95%.

## 2) Ultrasonic synthesis

The mixture of 0.01 mole of thiourea, substituted aromatic aldehydes (0.01 mole) and ethyl acetoacetate (0.01 mole) is added into a beaker containing 10 ml of ethanol and subjected for ultra-sonication in an ultra sonicator at 220 Hz for requisite time until the completion of reaction. Checked by TLC. Filtered and recrystallized to offer title compounds.

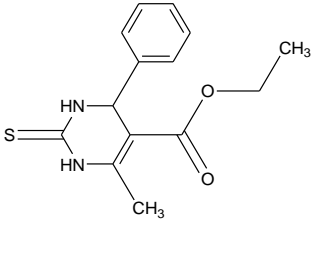
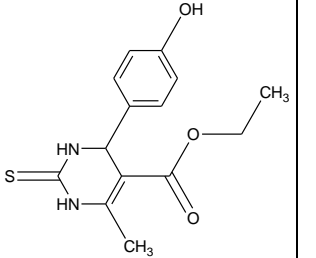
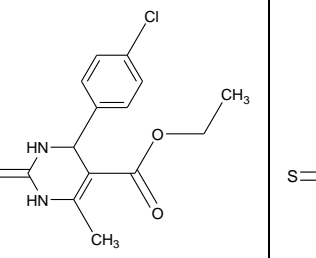
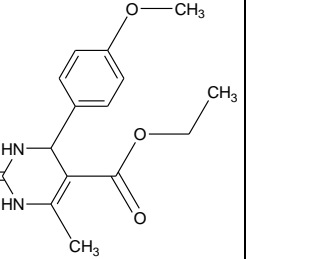
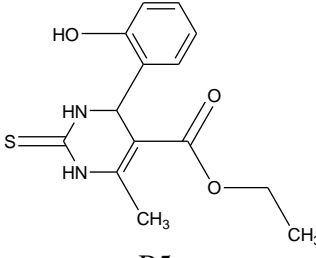
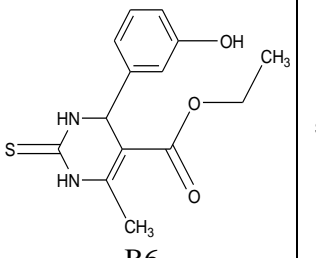
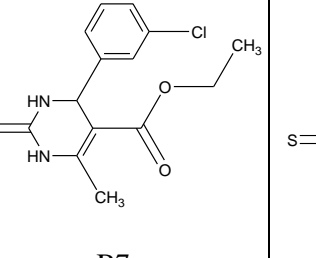
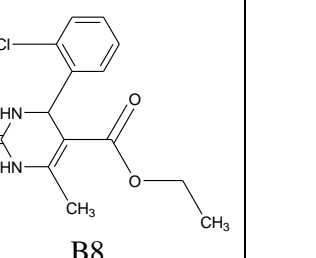
## 3) Microwave synthesis

The mixture of 0.01 mole of thiourea, substituted aromatic aldehydes (0.01 mol) and ethyl acetoacetate (0.01 mol) is added into a RBF containing 10 ml of ethanol and subjected for Microwave irradiation at 160W in a microwave reactor for requisite time until the completion of reaction was checked by TLC. The product formed was filtered and recrystallized to offer title compounds. The proposed reaction scheme for the synthesis of 1, 2, 3, 4-tetrahydropyrimidine derivatives is depicted in Fig 2 and the structures of the synthesized compounds are tabulated in Table 1 along with physicochemical parameters of synthesized compounds depicted in Table 2. The table 3 indicates the comparative data for the three methods of synthesis of tetrahydropyrimidine-2-one compound.



**Fig 2.** The proposed reaction scheme for the synthesis of 1,2,3,4-tetrahydropyrimidine derivatives

**Table1.** Structures of the synthesized compounds

			
<b>B1</b>	<b>B2</b>	<b>B3</b>	<b>B4</b>
			
<b>B5</b>	<b>B6</b>	<b>B7</b>	<b>B8</b>

**Table 2.** Physicochemical parameters of synthesized compounds

Comp.	Mol. Formula	Appearance	M.P.( <sup>o</sup> C)	Rf value	Elemental Analyses calculated		
					C	H	N
B1	C <sub>14</sub> H <sub>16</sub> N <sub>2</sub> O <sub>2</sub> S	Brownish yellow	145-149	0.51	60.85	5.84	10.14
B2	C <sub>14</sub> H <sub>16</sub> N <sub>2</sub> O <sub>3</sub> S	orange	157-163	0.67	57.52	5.52	9.58
B3	C <sub>14</sub> H <sub>15</sub> ClN <sub>2</sub> O <sub>2</sub> S	Yellow	149-156	0.78	54.10	4.86	9.01
B4	C <sub>15</sub> H <sub>18</sub> N <sub>2</sub> O <sub>3</sub> S	Yellow	161-167	0.49	58.80	5.92	9.14
B5	C <sub>14</sub> H <sub>16</sub> N <sub>2</sub> O <sub>3</sub> S	pale Yellow	179-184	0.48	57.52	5.52	9.58
B6	C <sub>14</sub> H <sub>16</sub> N <sub>2</sub> O <sub>3</sub> S	Brownish yellow	185-187	0.79	57.52	5.52	9.58
B7	C <sub>14</sub> H <sub>15</sub> ClN <sub>2</sub> O <sub>2</sub> S	off-white	179-189	0.65	54.10	4.86	9.01
B8	C <sub>14</sub> H <sub>15</sub> ClN <sub>2</sub> O <sub>2</sub> S	orange	156-178	0.80	54.10	4.86	9.01

**Table 3.** Comparative data for the three methods of synthesis of tetrahydropyrimidine-2-one compound

Comp.	Time required for synthesis(Min.)			Percent practical yield (%)		
	Conventional	Ultrasonic	Microwave	Conventional	Ultrasonic	Microwave
B1	92	37	3	56.43	56.20	75.45
B2	106	34	2	68.67	47.34	79.70
B3	95	39	1	57.58	63.56	80.50
B4	109	42	4	89.56	70.43	75.14
B5	99	38	3	80.67	69.70	86.40
B6	89	40	5	96.21	78.90	74.32
B7	79	33	2	62.89	69.09	79.55
B8	100	41	2	75.34	94.45	69.00

**Spectral Interpretation of Synthesized Compounds (Microwave method)****B1. [ethyl 1,2,3,4-tetrahydro-6-methyl-4-phenyl-2-thioxopyrimidine-5-carboxylate]**

Molecular weight: 276.35 gm/mol.  $^1\text{H}$  NMR ( $\text{CHCl}_3\text{-}d_6$  400 MHz)  $\delta$  ppm: 1.40 (t,  $-\text{CH}_3$  of Acetate),  $\square$  1.70(s  $-\text{CH}_3$ ), 2.2 (s-NH of pyridine)  $\square$  4.13(d,  $-\text{CH}_2$  of methyl),  $\square$  4.29 (s, -methine),  $\square$  6.03 (s, -NH of thiourea),  $\square$  6.90, 6.34, 6.67, 6.34(m, Ar).  $^{13}\text{C}$  NMR ( $\text{CHCl}_3\text{-}d_6$  400 MHz)  $\delta$  ppm: 14.12, 15.34, 53.29, 63.98, 109.65, 125.56, 126.30, 130.56, 146.34, 162.34, 176.45. MS: m/z 275.08, 276.98 (m+1), 277.12 (m+2).

**B2. [ethyl 1,2,3,4-tetrahydro-4-(4-hydroxyphenyl)-6-methyl-2-thioxopyrimidine-5-carboxylate]**

Molecular weight: 292.35 gm/mol.  $^1\text{H}$  NMR ( $\text{CHCl}_3\text{-}d_6$  400 MHz)  $\delta$  ppm: 1.20 (t,  $-\text{CH}_3$  of Acetate),  $\square$  1.69(s  $-\text{CH}_3$ ), 2.1(s-NH of pyridine)  $\square$  4.12 (d,  $-\text{CH}_2$  of methyl),  $\square$  4.49 (s, -methine),  $\square$  6.41 (s, -NH of thiourea),  $\square$  6.60, 6.70, 6.67, 6.80 (q, Ar).  $^{13}\text{C}$  NMR ( $\text{CHCl}_3\text{-}d_6$  400 MHz)  $\delta$  ppm: 14.03, 15.04, 53.29, 63.98, 105.34, 117.65, 126.56, 137.30, 154.56, 167.34, 172.34. MS: m/z 292.04, 293.93 (m+1), 294.12 (m+2).

**B3. [ethyl 4-(4-chlorophenyl)-1,2,3,4-tetrahydro-6-methyl-2-thioxopyrimidine-5-carboxylate]**

Molecular weight: 310.08 gm/mol,  $^1\text{H}$  NMR ( $\text{CHCl}_3\text{-}d_6$  400 MHz)  $\delta$  ppm: 1.32(t,  $-\text{CH}_3$  of Acetate),  $\square$  1.74 (s  $-\text{CH}_3$ ), 2.3 (s-NH of pyridine)  $\square$  4.22 (d,  $-\text{CH}_2$  of methyl),  $\square$  4.50 (s -methine),  $\square$  2.3 (s, -NH of thiourea),  $\square$  6.60, 6.70, 6.67, 6.80 (q, Ar).  $^{13}\text{C}$  NMR ( $\text{CHCl}_3\text{-}d_6$  400 MHz)  $\delta$  ppm: 14.23, 15.34, 55.39, 63.98, 106.84, 124.65, 133.56, 142.30, 160.56, 164.34, 172.34, MS: m/z 310.12, 311.85 (m+1), 313.09 (m+2).

**B4. [ethyl 1,2,3,4-tetrahydro-4-(4-methoxyphenyl)-6-methyl-2-thioxopyrimidine-5-carboxylate]**

Molecular weight: 306.38 gm/mol,  $^1\text{H}$  NMR ( $\text{CHCl}_3\text{-}d_6$  400 MHz)  $\delta$  ppm: 1.35 (t,  $-\text{CH}_3$  of Acetate),  $\square$  1.70 (s  $-\text{CH}_3$ ), 2.7 (s-NH of pyridine)  $\square$  4.20 (d,  $-\text{CH}_2$  of methyl), 4.56 (s -methine),  $\square$  6.56 (s, -NH of thiourea),  $\square$  6.63, 6.63, 6.90, 6.80 (q, Ar).  $^{13}\text{C}$  NMR ( $\text{CHCl}_3\text{-}d_6$  400 MHz)  $\delta$  ppm: 14.03, 15.84, 55.39, 57.98, 60.89, 106.84, 117.65, 129.56, 133.56, 157.30, 160.56, 164.34, 172.34. MS: m/z 308.41, 309.83 (m+1), 310.02 (m+2).

**In vitro Biological Evaluation**

Various concentrations of derivatives were prepared in DMSO to assess their antibacterial and antifungal activities against standard strains using broth dilution. Bacteria were maintained, and

drugs were diluted in nutrient Mueller Hinton broth. The broth was inoculated with  $10^8$  colony-forming units (cfu) per milliliter of test strains (Institute of Microbial Technology, Chandigarh, India) determined by turbidity. Stock solutions of synthesized derivate (2 mg/mL) were serially diluted for primary and secondary screening. The primary screen included 1000, 500, and 250  $\mu\text{g/mL}$  of synthesized derivatives, then those with activity were further screened at 200, 100, 50, 25, 12.5, and 6.250  $\mu\text{g/mL}$ . A control without antibiotic was sub-cultured (before inoculation) by spreading one loopful evenly over a quarter of a plate of medium suitable for growing test organisms and incubated at  $37^\circ\text{C}$  overnight. The lowest concentrations of derivatives that inhibited bacterial or fungal growth were taken as minimal inhibitory concentrations (MICs). These were compared with the amount of control growth before incubation (original inoculum) to determine MIC accuracy. The standards for antibacterial activity were gentamycin, ampicillin, chloramphenicol, ciprofloxacin, and norfloxacin served, and those for antifungal activity were nystatin and griseofulvin. The antimalarial behavior was tested using plasmodium falciparum, with quinine and chloroquine as the standards(27,28). Both experiments took place at the Microcare laboratory and Tuberculosis Research Centre [TRC] in Surat, Gujarat.

## Results

Pharmacokinetic characteristics are critical to drug development because they enable scientists to investigate the biological impacts of possible pharmacological candidates(29). This compound's oral bioavailability was evaluated using Lipinski's rule of five and Veber's rules (Table 4). To better understand the pharmacokinetics profiles and drug-likeness properties of the proposed compounds, the ADME characteristics of all of them were examined (Table 5). Fig. 3 depicts the physicochemical domain that is ideal for oral bioavailability. The oral acute toxicity have been predicted along with  $\text{LD}_{50}$  (mg/kg), toxicity class, hepatotoxicity, carcinogenicity, immunotoxicity, mutagenicity, and cytotoxicity (Table 6). Table 7 lists the ligand energies (kcal/mol), docking scores (kcal/mol), active amino acids, bond length ( $\text{\AA}$ ), and different interactions of derivatives with DHFR. Table 8 depicts the most potent compounds' 2D and 3D docking orientations. The results of antimicrobial and antifungal activities of the synthesized derivatives are tabulated in Table 9 which shows the MICs and MFCs respectively.

**Table 4.** Lipinski rule of 5 and Veber's rule calculated for molecules



Compound	Lipinski rule of five					Veber's rule	
	Log P	Mol. Wt.	HBA	HBD	Violations	Total polar surface area ( $\text{\AA}^2$ )	No. of rotatable bonds
NL	0.70	443.45	7	6	2	187.50	10
B1	1.51	276.35	2	2	0	82.45	4
B2	0.95	292.35	3	3	0	102.68	4
B3	2.03	310.8	2	2	0	82.45	4
B4	1.2	306.38	3	2	0	91.68	5
B5	0.95	292.35	3	3	0	102.68	4
B6	0.95	292.35	3	3	0	102.68	4
B7	2.03	310.8	2	2	0	82.45	4
B8	2.03	310.8	2	2	0	82.45	4

Where: Mol. Wt., molecular weight; HBA, hydrogen bond acceptors; HBD, hydrogen bond donors

**Table 5.** The pharmacokinetics and drug-likeness properties of developed compounds

Comp codes	Pharmacokinetics									Drug-likeness			
	GI abs.	BBB pen.	P-gp sub.	CYP1A2	CYP2C19	CYP2C9	CYP2D6	CYP3A4	Log $K_p$ (skin permeation, cm/s)	Ghose	Egan	Muegge	Bioavailability Score
				inhibitors									
NL	Low	No	Yes	No	No	No	No	No	-8.81	0	1	2	0.11
B1	High	No	No	Yes	Yes	Yes	No	No	-6.58	0	0	0	0.55
B2	High	No	No	No	Yes	No	No	No	-6.93	0	0	0	0.55
B3	High	No	No	Yes	Yes	Yes	No	Yes	-6.34	0	0	0	0.55
B4	High	No	No	Yes	Yes	Yes	No	No	-6.78	0	0	0	0.55
B5	High	No	No	No	Yes	No	No	No	-6.93	0	0	0	0.55
B6	High	No	No	No	Yes	No	No	No	-6.93	0	0	0	0.55
B7	High	No	No	Yes	Yes	Yes	No	Yes	-6.34	0	0	0	0.55
B8	High	No	No	Yes	Yes	Yes	No	Yes	-6.34	0	0	0	0.55

Where: NL, Native ligand; GI abs., gastrointestinal absorption; BBB pen., blood brain barrier penetration; P-gp sub., p-glycoprotein substrate

**Table 6.** The predicted acute toxicity of molecules

Comp d. codes	Parameters							
	LD <sub>50</sub> (mg/kg)	Tox class	Prediction accuracy (%)	Hepatotoxicity	Carcinogenicity	Immunotoxicity	Mutagenicity	Cytotoxicity
NL	135	3	67.38	I (0.87)	I (0.51)	I (0.99)	I (0.75)	I (0.63)
B1	785	4	54.26	I (0.51)	A(0.52)	I (0.99)	I (0.65)	I (0.74)
B2	785	4	54.26	A (0.51)	A(0.50)	I (0.99)	I (0.69)	I (0.83)
B3	785	4	54.26	I (0.53)	A(0.52)	I (0.99)	I (0.65)	I (0.74)
B4	785	4	54.26	I (0.50)	I (0.51)	I (0.99)	I (0.65)	I (0.86)
B5	150	3	54.26	A (0.51)	A(0.50)	I (0.99)	I (0.69)	I (0.86)
B6	150	3	54.26	A (0.51)	A(0.50)	I (0.99)	I (0.69)	I (0.83)
B7	785	4	54.26	I (0.53)	A(0.52)	I (0.99)	I (0.65)	I (0.74)
B8	250	3	54.26	I (0.55)	A(0.51)	I (0.99)	I (0.65)	I (0.75)

Where: I, Inactive; A, Active

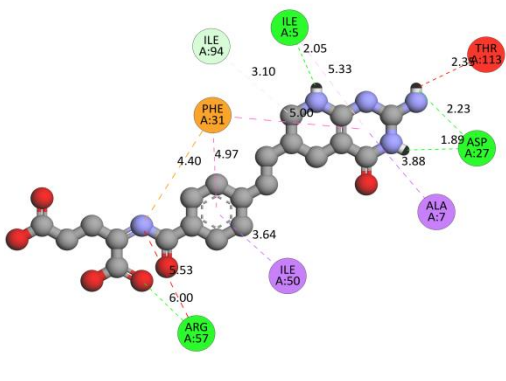
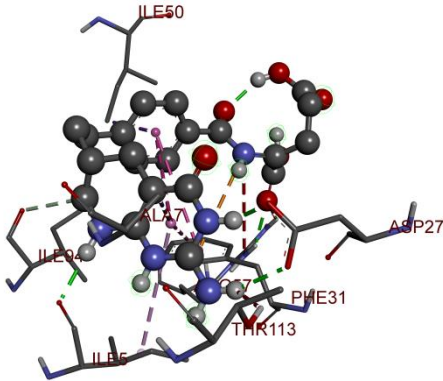
**Table 7.** The ligand energies (kcal/mol), docking scores (kcal/mol), active amino acids, bond length (Å), and different interactions of derivatives with DHFR

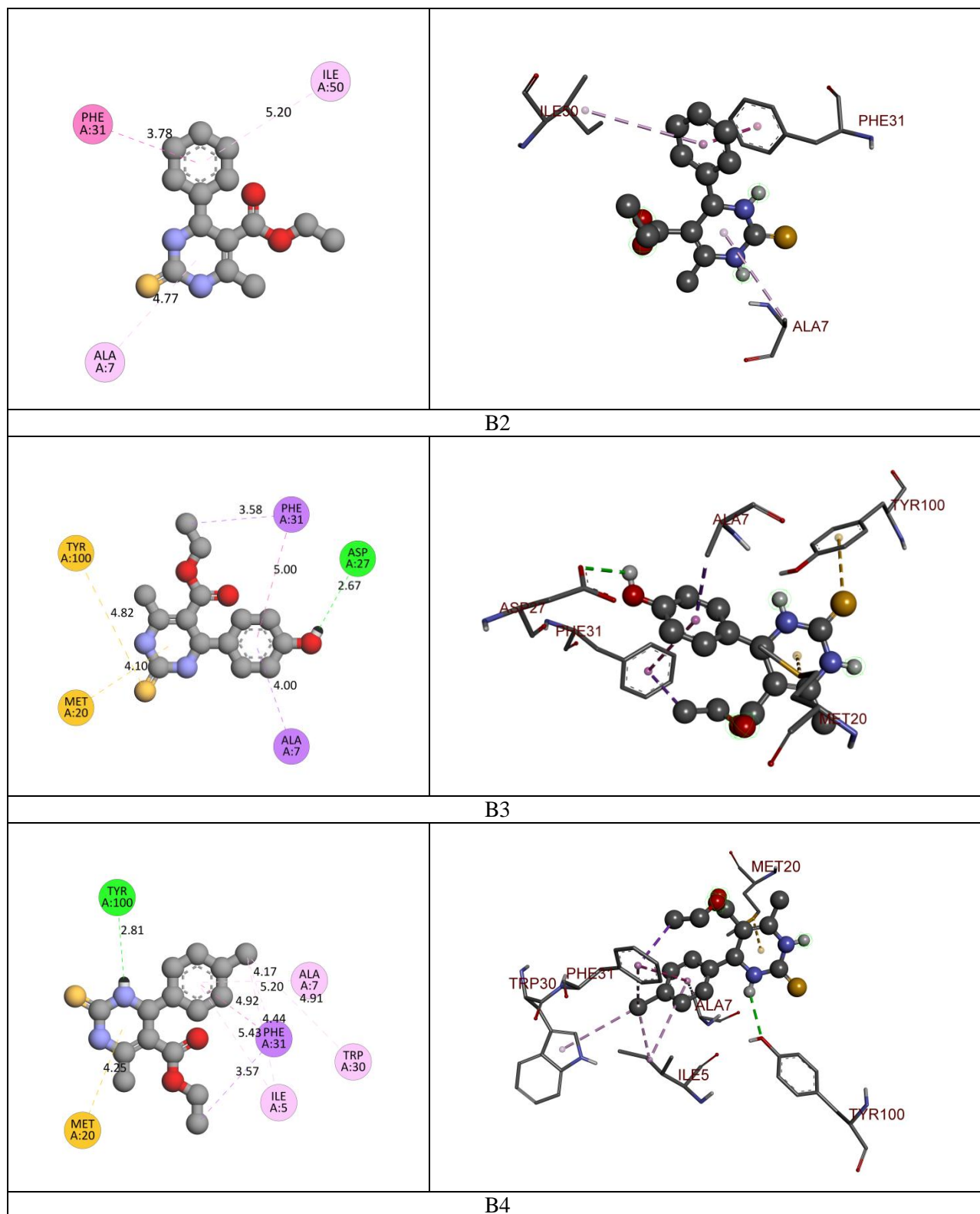
Active Amino Acid	Bond Length	Bond Type	Bond Category	Ligand Energy	Binding Affinity
B1					
PHE31	3.7795	Hydrophobic	Pi-Pi Stacked	241.91	-7.3
ALA7	4.76998		Pi-Alkyl		
ILE50	5.19917				
B2					
ASP27	2.6667	Hydrogen Bond	Conventional Hydrogen Bond	245.67	-7.6
PHE31	3.57726	Hydrophobic	Pi-Sigma		
ALA7	3.99812		Other		
TYR100	4.82196	Pi-Pi T-shaped			
MET20	4.10189				
PHE31	4.99648	Hydrophobic	Pi-Pi T-shaped		
B3					
TYR100	2.81132	Hydrogen Bond	Conventional Hydrogen Bond	247.27	-7.5
PHE31	3.56996	Hydrophobic	Pi-Sigma		
MET20	4.24596	Other	Pi-Sulfur		
PHE31	4.92221	Hydrophobic	Pi-Pi T-shaped		
ILE5	4.44024		Alkyl		
	5.43		Pi-Alkyl		

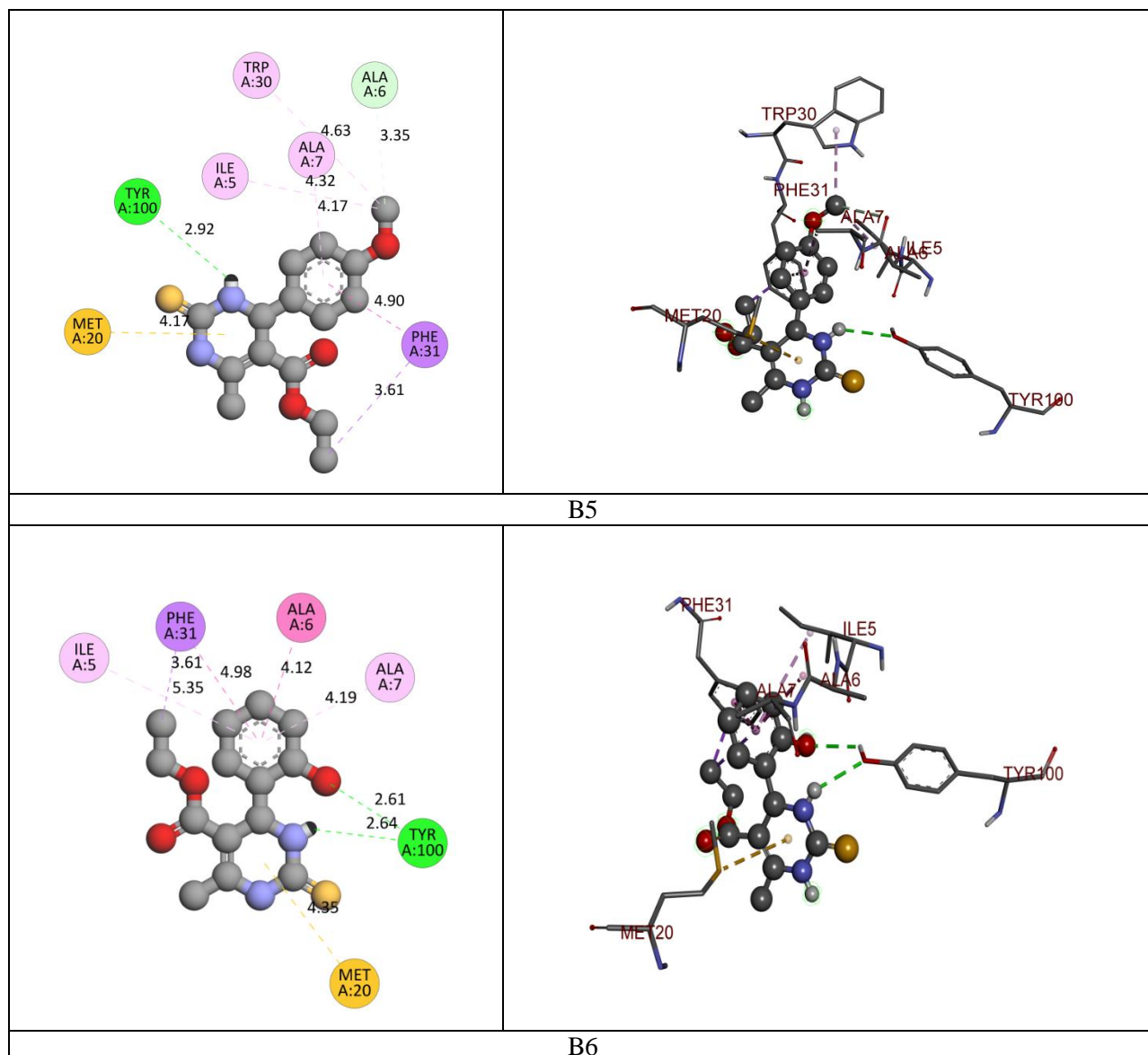
ALA7	4.16931				
TRP30	4.91129				
PHE31	5.19764				
B4					
TYR100	2.91731	Hydrogen Bond	Conventional Hydrogen Bond	255.85	-7.3
ALA6	3.35307		Carbon Hydrogen Bond		
PHE31	3.60754	Hydrophobic	Pi-Sigma		
MET20	4.16694	Other	Pi-Sulfur		
PHE31	4.89896	Hydrophobic	Pi-Pi T-shaped		
ILE5	4.32355		Alkyl		
ALA7	4.17052		Pi-Alkyl		
TRP30	4.6284				
B5					
TYR100	2.64394	Hydrogen Bond	Conventional Hydrogen Bond	267.37	-7.6
	2.60733				
	3.94554	Hydrophobic	Pi-Sigma		
PHE31	3.61464				
MET20	4.35489	Other	Pi-Sulfur		
PHE31	4.9767	Hydrophobic	Pi-Pi T-shaped		
ALA6,ALA7	4.11992		Amide-Pi Stacked		
ILE5	5.34502		Pi-Alkyl		
ALA7	4.19343				
B6					
GLY15	2.36118	Hydrogen Bond	Conventional Hydrogen Bond	241.89	-7.5
TYR100	5.0837	Other	Pi-Sulfur		
MET20	3.98859				
PHE31	4.67406	Hydrophobic	Pi-Pi T-shaped		
ILE50	4.12063		Alkyl		
LEU54	4.53693		Pi-Alkyl		
ILE5	5.37503				
ALA7	4.20986				
PHE31	4.25113				
B7					
PHE31	3.79388	Hydrophobic	Pi-Pi Stacked	245.67	-7.4
LEU28	3.84666		Alkyl		
ALA7	4.80228		Pi-Alkyl		
ILE50	5.1643				
LEU54	5.4762				

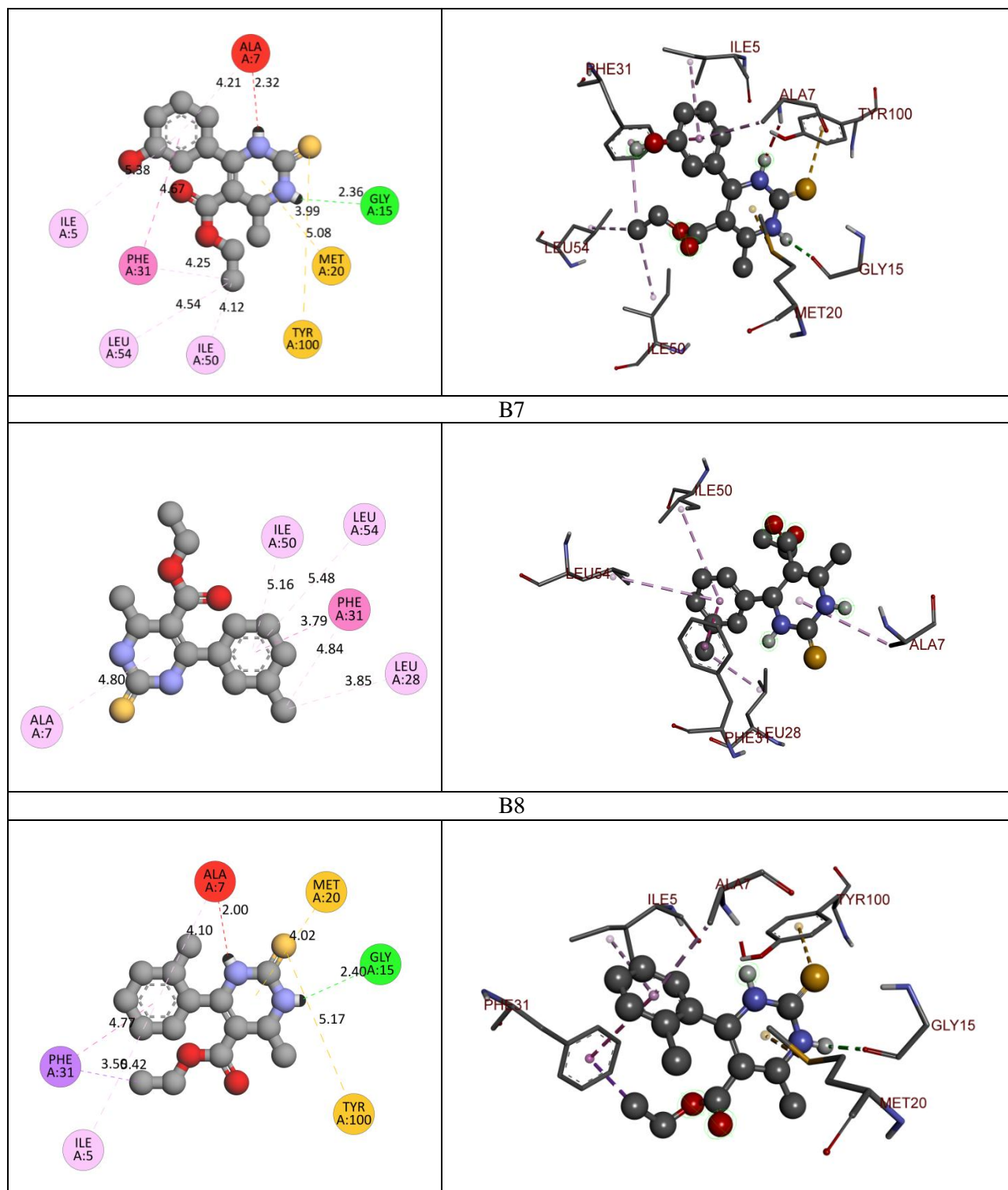
PHE31	4.84461						
B8							
GLY15	2.39635	Hydrogen Bond	Conventional Hydrogen Bond	286.62	-7.4		
PHE31	3.50021	Hydrophobic	Pi-Sigma				
TYR100	5.17181	Other	Pi-Sulfur				
MET20	4.02448						
PHE31	4.76693	Hydrophobic	Pi-Pi T-shaped				
ILE5	5.4177		Pi-Alkyl				
ALA7	4.10146						
NL							
ASP27	1.89071	Hydrogen Bond	Conventional Hydrogen Bond	293.4	-8.6		
	2.23099						
ILE5	2.04556		Carbon Hydrogen Bond				
	2.00364						
ARG57	2.14074		Pi-Cation				
	2.64414						
ILE94	3.10227	Electrostatic	Pi-Sigma				
PHE31	4.39543						
ALA7	3.87526		Pi-Pi T-shaped				
ILE50	3.63978						
	5.85001						
PHE31	4.96722						
	4.99602						

**Table 8.** The 2D- and 3D binding orientations of native ligand and molecules selected for the synthesis from virtual screening

2D-binding orientations	3D-binding orientations
Native ligand	
	
B1	





**Table 9.** The antimicrobial and antifungal activities of the synthesized derivatives

Compound code	Antimicrobial activity	Antifungal activity
---------------	------------------------	---------------------



	[MIC (µg/mL)]				[MFC (µg/mL)]		
	<i>E.C.</i>	<i>P.A.</i>	<i>S.A.</i>	<i>S.P.</i>	<i>C.A.</i>	<i>A.N.</i>	<i>A.C.</i>
B1	75	1.5	75	125	200	150	200
B2	125	50	50	150	100	150	175
B3	50	50	225	150	550	150	150
B4	145	150	225	0.75	100	150	150
B5	100	125	0.50	150	100	100	150
B6	30	50	50	150	550	125	200
B7	125	15	25	20	50	125	150
B8	05	15	50	20	125	125	150
Gentamycin	0.05	1	0.25	0.5	NA	NA	NA
Ampicillin	100	NA	250	100	NA	NA	NA
Chloramphenicol	50	50	50	50	NA	NA	NA
Ciprofloxacin	25	25	50	50	NA	NA	NA
Norfloxacin	10	10	10	10	NA	NA	NA
Nystatin	NA	NA	NA	NA	100	100	100
Greseofulvin	NA	NA	NA	NA	500	100	100

Where,

*E.C.*, *Escherichia coli*; *P.A.*, *Pseudomonas aeruginosa*; *S.A.*, *Staphylococcus aureus*; *S.P.*, *Staphylococcus pyogenes*; *C.A.*, *Candida albicans*; *A.N.*, *Aspergillus niger*; *A.C.*, *Aspergillus clavatus*; *MIC*, Minimum inhibitory concentration; *MFCs*, minimum fungicidal concentration, *NS*, Non-sensitive

## Discussion

In present study we have designed and developed some 1, 2, 3, 4-tetrahydropyrimidine derivatives as potential DHFR inhibitors. In accordance with Lipinski's and Veber's rule (Table 4), Native ligand has violated both the rules. The log P values of all the molecules were between the ranges -0.95 to 2.03 which indicates optimum lipophilicity. Lipophilicity is a significant feature of the molecule that affects how it works in the body(27). It is determined by the compound's Log P value, which measures the drug's permeability in the body to reach the target tissue(30,31). The molecular weight of all the molecules was below 500 Da which indicates active better transport of the molecules through biological membrane. Fortunately, the Lipinski rule of 5 had not been compromised by the compounds, excluding native ligand which displayed 2 violations of Lipinski rule respectively(28,29). The total polar surface area (TPSA) and the number of rotatable bonds have been found to better discriminate between compounds that are orally active or not. According to Veber's rule, TPSA should be  $\leq 140$  and number of rotatable bonds should be  $\leq 10$ . It was observed that native ligand violated the Veber's rule, as it has TPSA  $187.50 \text{ \AA}^2$  and number of rotatable bonds 10 which indicate its poor oral bioavailability.

In order to further optimize the compounds, pharmacokinetics and drug-likeness properties were calculated for each one. All the compounds including native ligand showed no penetration to the blood-brain barrier (BBB). The log  $K_p$  (skin penetration, cm/s) and bioavailability values of all the compounds were within acceptable limits. Native ligand do not meet all, two, or one of the Ghose, Egan, and Muegge requirements also showed lower GI absorption (Table 5).

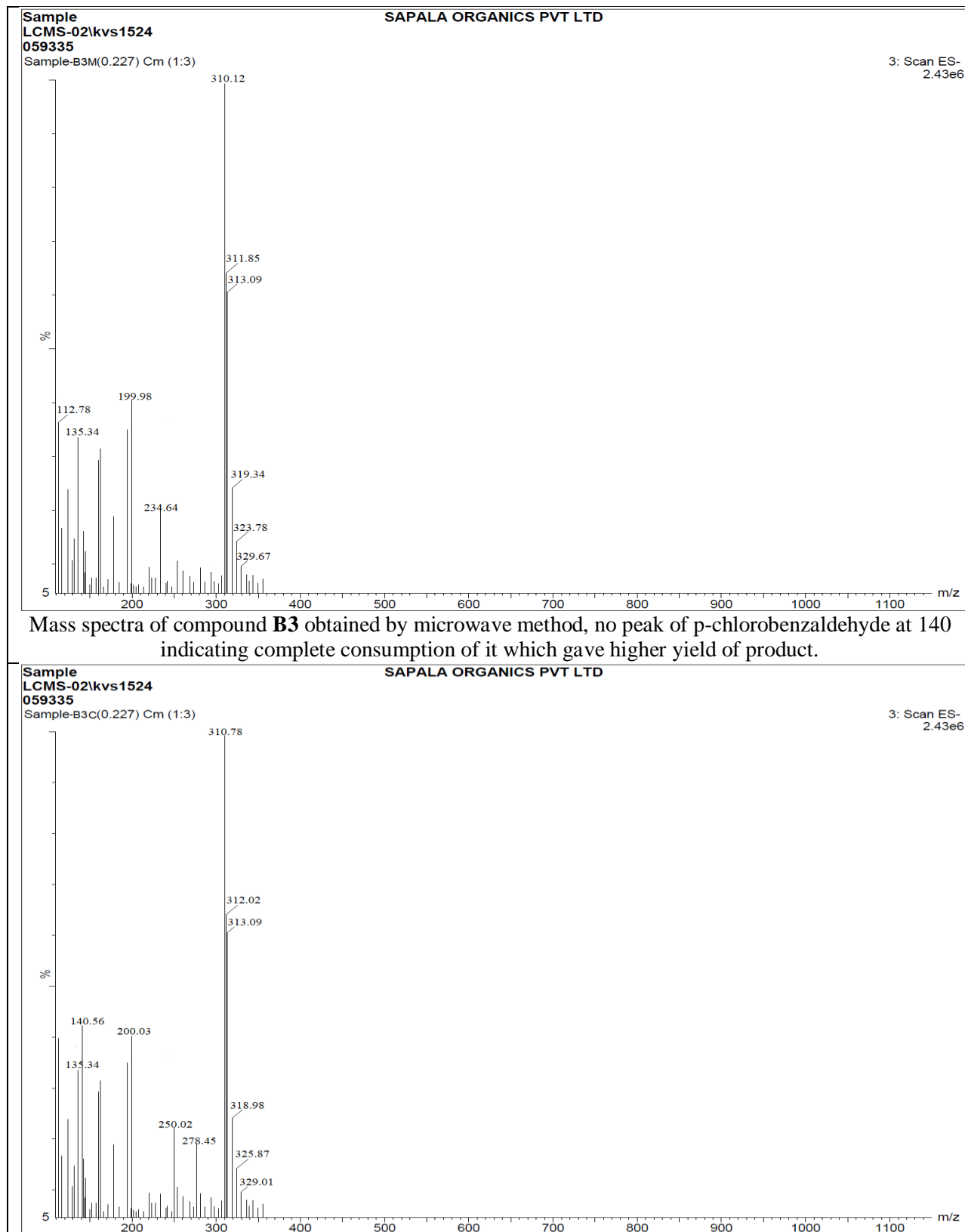
In acute toxicity predictions, native ligand and **B5**, **B6**, and **B8** fall in toxicity class-III i.e. toxic if swallowed ( $50 < LD_{50} \leq 300$ ). Molecules **B1**, **B2**, **B3**, **B4** and **B7** displayed toxicity class-IV which means harmful if swallowed ( $300 < LD_{50} \leq 2000$ ) (17). From this virtual screening, it was concluded that all the compounds possess drug-like properties and hence were subjected to molecular docking studies.

The binding affinities of the derivatives have been compared with the binding mode of native ligand present in the crystal structure of DHFR (PDB ID: 5CCC). Native ligand exhibited -8.6 kcal/mol binding affinity with DHFR and formed 6 conventional hydrogen bonds with Asp27, Ile5, Arg57 and one carbon-hydrogen bond with Ile94. It has developed many hydrophobic interactions such as Pi-cation, Pi-sigma, Pi-Pi T-shaped and Pi-alkyl bonds with Phe31, Ala7, Ile50, and Ile5.

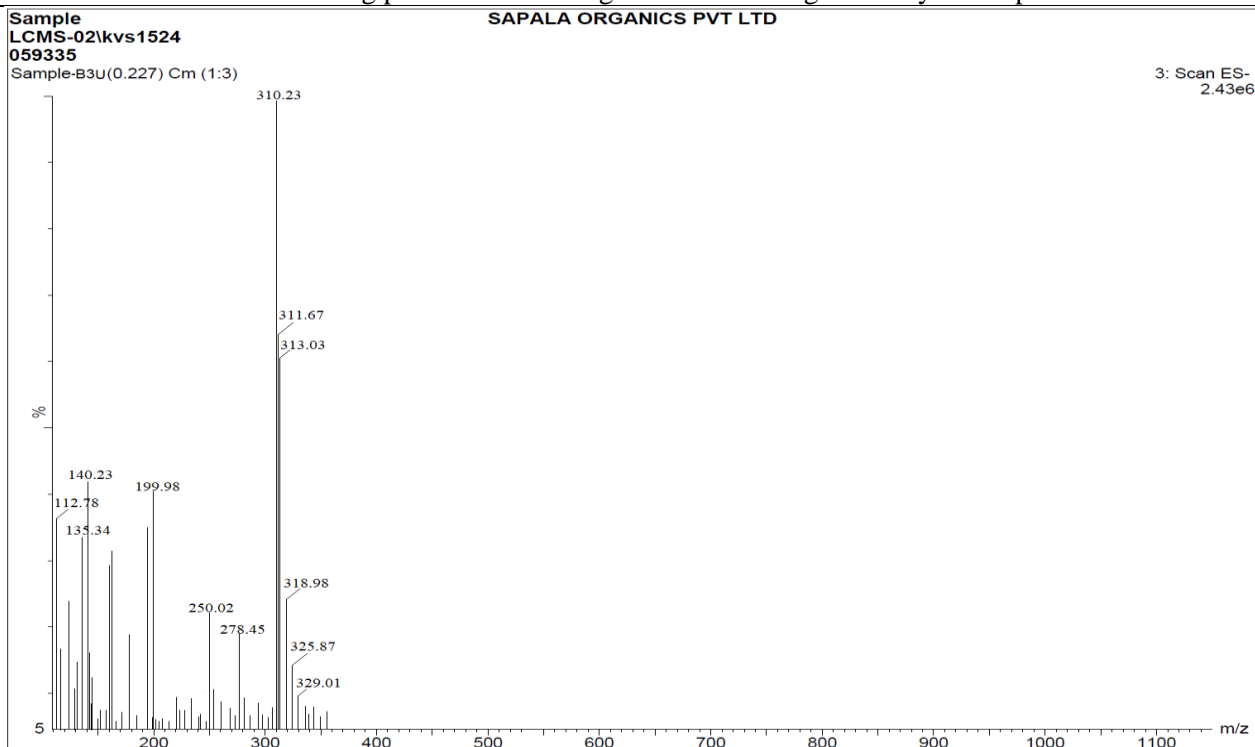
Compound **B1** exhibited -7.3 kcal/mol binding affinity, developed Pi-pi stacked and Pi-alkyl hydrophobic interactions with Phe31, Ala7 and Ile5. Compound **B2** displayed -7.6 kcal/mol binding affinity, also formed one conventional hydrogen bond with ASP27, whereas developed hydrophobic interactions with Phe31 & Ala7. Compound **B3** and **B5** exhibited -7.5 kcal/mol binding affinity, formed two conventional hydrogen bonds with Tyr100, Phe31, Met20 & Ile5 whereas it has developed Pi-sigma, pi-sulfurhydrophobic bonds with Phe31 & Ile5. Compound **B4** displayed -7.3 kcal/mol binding affinity, formed two hydrogen bonds, conventional & carbon with Tyr100 & Ala6 whereas it has developed one Pi-sigma Pi-sulfur hydrophobic bonds with Phe31 and Met20, Pi-Pi T-shaped & Pi-Alkyl hydrophobic bonds with Phe31 & Ala7. Molecules **B7** & **B8** exhibited -7.4 kcal/mol binding affinity developed one conventional type of hydrogen

bond, whereas formed Pi-Pi T-shaped, Pi-Pi Stacked & Pi-Sigma type of hydrophobic Interactions with Phe31, Tyr100 & Met20.

Although the compounds were synthesized by three methods and the progression of reaction was monitored by TLC, we have investigated the most effective method suitable for the synthesis which can give maximum yield and consumed complete starting material. We have subjected one compound for mass study to check which method can still have starting material peak in the crude obtained product. Compound **B3** was selected to prove comparative effectiveness of the method in which p-chlorobenzaldehyde was used as substituent. For the synthesis of compound **B3**, it took 95, 39, and 1 min to complete the reaction through conventional, ultrasonic, and microwave method respectively. It was also observed that yield of the compound was very good in microwave assisted synthesis i.e. 80.50% which is almost 30-40% more than that of the conventional and ultrasonic method. In mass spectrum it was observed that, product obtained through microwave method was completely pure and did not display any peak of starting material, whereas product obtained through conventional and ultrasonic method showed presence of starting material. It means even after taking much time for the reaction and consuming more energy starting material did not get consumed in these both methods which ultimately affected on their product yield. A detailed comparative mass analysis of compound is explained in Fig. 3.



Mass spectra of compound **B3** obtained by conventional method, showing peak of p-chlorobenzaldehyde at 139.72 indicating presence of starting material which gave less yield of product.



Mass spectra of compound **B3** obtained by ultrasonic method, showing peak of p-chlorobenzaldehyde at 140.23 indicating presence of starting material which gave less yield of product.

**Fig. 3.** Comparative mass spectrum analysis of compound **B3** synthesized by conventional, ultrasonic and microwave method

Millions of humans are now affected by bacterial diseases triggered by pathogenic bacteria which are responsible for elevated child mortality rates in developed countries. Not all bacteria are pathogenic. For example, there are thousands of bacterial organisms in the human digestive tract, some of which are harmless and even useful. Furthermore, various mechanisms of action on the target site can aid in the discovery of potential drugs while developing antibacterial agents. However, since bacteria have developed antibiotic tolerance, finding a new antibacterial agent became difficult. Gram-positive bacteria, such as *methicillin-resistant S. aureus*, *S. epidermis*, *vancomycin-resistant E. calcium*, and *penicillin-resistant S. pneumoniae*, induce the majority of bacterial infections. Fungal infections have become more frequent, and the majority of them are minor. There are various varieties of fungi that cause infections today(27,28). Species like *candida* and *aspergillus* are only a few examples. In present

investigation, all the synthesized compounds were subjected for *in vitro* antibacterial and antifungal activity using different strains as given in Table 9.

All the synthesized compounds were sensitive to gram +ve(*Staphylococcus aureus*, *Staphylococcus pyogenes*) and gram –ve(*Escherichia coli*, *Pseudomonas aeruginosa*) bacterial strains. All the compounds demonstrated more potent activity than Ampicillin against both gram-positive and gram-negative bacteria. All the compounds **B1-B8** were sensitive against *Staphylococcus aureus* strains & found to be more potent than the standard drug Ampicillin. Compounds **B1, B3, & B6** were sensitive at 75, 50 & 30 µg/mL against *Escherichia coli*. All the In antifungal activity, compound **B7** was found to be more potent with MFCs 50 µg/mL against *Candida albicans*. It can be concluded that substitution at meta-position with bulky group can greatly increase the activity of the designed compounds.

## Conclusion

Dihydrofolate reductase (DHFR) is an important enzyme required to maintain bacterial growth, and hence inhibitors of DHFR have been proven as effective agents for treating bacterial infections. In present study we have designed and developed some 1, 2, 3, 4-tetrahydropyrimidine derivatives as potential DHFR inhibitors. The designed derivatives were screened through Lipinski rule, Veber's rule, ADMET analysis, drug-likeness properties, and molecular docking. The selected derivatives were synthesized and subjected for *in vitro* biological evaluation. It was also observed that yield of the compound was very good in microwave assisted synthesis i.e. 80.50% which is almost 30-40% more than that of the conventional and ultrasonic method. In mass spectrum it was observed that, product obtained through microwave method was completely pure and did not displayed any peak of starting material, whereas product obtained through conventional and ultrasonic method showed presence of starting material. Therefore we concluded that the microwave assisted synthesis method is most suitable for the synthesis of tetrahydropyrimidine derivatives through Biginelli reaction. We hereby report that, all the compounds **B1, B2, B3, B4, B5, B6, B7** and **B8** were found to be are potent and can be developed further to get more promising molecules for the treatment of bacterial & fungal infections.

## References

1. Murali TS, Kavitha S, Spoorthi J, Bhat D V., Prasad ASB, Upton Z, et al. Characteristics of microbial drug resistance and its correlates in chronic diabetic foot ulcer infections. *J Med Microbiol*. 2014;63:1377–85.
2. Sánchez-Sánchez M, Cruz-Pulido WL, Bladinieres-Cámara E, Alcalá-Durán R, Rivera-Sánchez G, Bocanegra-García V. Bacterial Prevalence and Antibiotic Resistance in Clinical Isolates of Diabetic Foot Ulcers in the Northeast of Tamaulipas, Mexico. *Int J Low Extrem Wounds*. 2017;16(2):129–34.
3. Loi V Van, Huyen NTT, Busche T, Tung QN, Gruhlke MCH, Kalinowski J, et al. *Staphylococcus aureus* responds to allicin by global S-thioallylation – Role of the Brx/BSH/YpdA pathway and the disulfide reductase MerA to overcome allicin stress. *Free Radic Biol Med*. 2019;139:55–69.
4. Jouhar L, Jaafar RF, Nasreddine R, Itani O, Haddad F, Rizk N, et al. Microbiological profile and antimicrobial resistance among diabetic foot infections in Lebanon. *Int Wound J*. 2020;17(6):1764–73.
5. Anwar K, Hussein D, Salih J. Antimicrobial susceptibility testing and phenotypic detection of MRSA isolated from diabetic foot infection. *Int J Gen Med*. 2020;13:1349–57.
6. Wróbel A, Arciszewska K, Maliszewski D, Drozdowska D. Trimethoprim and other nonclassical antifolates an excellent template for searching modifications of dihydrofolate reductase enzyme inhibitors. *J Antibiot (Tokyo)*. 2020;73(1):5–27.
7. Todd MJ, Gomez J. Enzyme kinetics determined using calorimetry: A general assay for enzyme activity? *Anal Biochem*. 2001;296(2):179–87.
8. Shahi SK, Kumar A. Isolation and genetic analysis of multidrug resistant bacteria from diabetic foot ulcers. *Front Microbiol*. 2016;6(JAN).
9. Nepali K, Sharma S, Sharma M, Bedi PMS, Dhar KL. Rational approaches, design strategies, structure activity relationship and mechanistic insights for anticancer hybrids. *Eur J Med Chem* [Internet]. 2014;77:422–87. Available from: <http://dx.doi.org/10.1016/j.ejmech.2014.03.018>
10. Nerkar AU. Use of Pyrimidine and Its Derivative in Pharmaceuticals: A Review. *J Adv Chem Sci*. 2021;7(2):729–32.
11. Mittersteiner M, Farias FFS, Bonacorso HG, Martins MAP, Zanatta N. Ultrasound-assisted synthesis of pyrimidines and their fused derivatives: A review. *Ultrason Sonochem*. 2021;79.
12. Verma V, Joshi CP, Agarwal A, Soni S, Kataria U. A Review on Pharmacological Aspects of Pyrimidine Derivatives. *J Drug Deliv Ther*. 2020;10(5):358–61.

13. Ahmed Elkanzi NA. Synthesis and Biological Activities of Some Pyrimidine Derivatives: A Review. *Orient J Chem*. 2020;36(6):1001–15.
14. Bhat AR, Dongre RS, Naikoo GA, Hassan IU, Ara T. Proficient synthesis of bioactive annulated pyrimidine derivatives: A review. *J Taibah Univ Sci*. 2017;11(6):1047–69.
15. Kim S, Chen J, Cheng T, Gindulyte A, He J, He S, et al. PubChem in 2021: New data content and improved web interfaces. *Nucleic Acids Res*. 2021;49(D1):D1388–95.
16. Daina A, Michielin O, Zoete V. SwissADME: A free web tool to evaluate pharmacokinetics, drug-likeness and medicinal chemistry friendliness of small molecules. *Sci Rep*. 2017;7.
17. Banerjee P, Eckert AO, Schrey AK, Preissner R. ProTox-II: A webserver for the prediction of toxicity of chemicals. *Nucleic Acids Res*. 2018;46(W1):W257–63.
18. Dallakyan S, Olson AJ. Small-molecule library screening by docking with PyRx. *Methods Mol Biol*. 2015;1263(1263):243–50.
19. Rappé AK, Casewit CJ, Colwell KS, Goddard WA, Skiff WM. UFF, a Full Periodic Table Force Field for Molecular Mechanics and Molecular Dynamics Simulations. *J Am Chem Soc*. 1992;114(25):10024–35.
20. San Diego: Accelrys Software Inc. Discovery Studio Modeling Environment, Release 3.5. Accelrys Softw Inc [Internet]. 2012; Available from: <https://www.3dsbiovia.com/about/citations-references/>
21. Khan SL, Siddiqui FA, Jain SP, Sonwane GM. Discovery of Potential Inhibitors of SARS-CoV-2 (COVID-19) Main Protease (Mpro) from Nigella Sativa (Black Seed) by Molecular Docking Study. *Coronaviruses*. 2020;2(3):384–402.
22. Chaudhari RN, Khan SL, Chaudhary RS, Jain SP, Siddiqui FA. B-Sitosterol: Isolation from Muntingia Calabura Linn Bark Extract, Structural Elucidation And Molecular Docking Studies As Potential Inhibitor of SARS-CoV-2 Mpro (COVID-19). *Asian J Pharm Clin Res*. 2020;13(5):204–9.
23. Khan SL, Siddiqui FA, Shaikh MS, Nema N V., Shaikh AA. Discovery of potential inhibitors of the receptor-binding domain (RBD) of pandemic disease-causing SARS-CoV-2 Spike Glycoprotein from Triphala through molecular docking. *Curr Chinese Chem* [Internet]. 2021;01. Available from: <https://www.eurekaselect.com/192390/article>
24. Khan SL, Sonwane GM, Siddiqui FA, Jain SP, Kale MA, Borkar VS. Discovery of Naturally Occurring Flavonoids as Human Cytochrome P450 (CYP3A4) Inhibitors with the Aid of Computational Chemistry. *Indo Glob J Pharm Sci*. 2020;10(04):58–69.



25. Siddiqui FA, Khan SL, Marathe RP, Nema N V. Design, Synthesis, and In Silico Studies of Novel N-(2-Aminophenyl)-2,3- Diphenylquinoxaline-6-Sulfonamide Derivatives Targeting Receptor-Binding Domain (RBD) of SARS-CoV-2 Spike Glycoprotein and their Evaluation as Antimicrobial and Antimalarial Agents. *Lett Drug Des Discov* [Internet]. 2021;18(9):915–31. Available from: <https://doi.org/10.2174/1570180818666210427095203>
26. Shen ZL, Xu XP, Ji SJ. Brønsted base-catalyzed one-pot three-component Biginelli-type reaction: An efficient synthesis of 4,5,6-triaryl-3,4-dihydropyrimidin-2(1H)-one and mechanistic study. *J Org Chem*. 2010;75(4):1162–7.
27. Khan S, Kale M, Siddiqui F, Nema N. Novel pyrimidine-benzimidazole hybrids with antibacterial and antifungal properties and potential inhibition of SARS-CoV-2 main protease and spike glycoprotein. *Digit Chinese Med*. 2021;4(2):102–19.
28. Shntaif AH, Khan S, Tapadiya G, Chettupalli A, Saboo S, Shaikh MS, et al. Rational drug design, synthesis, and biological evaluation of novel N-(2-arylamino phenyl)-2,3-diphenylquinoxaline-6-sulfonamides as potential antimalarial, antifungal, and antibacterial agents. *Digit Chinese Med* [Internet]. 2021;4(4):290–304. Available from: <https://www.sciencedirect.com/science/article/pii/S2589377721000483>
29. Khan A, Unnisa A, Sohel M, Date M, Panpaliya N, Saboo SG, et al. Investigation of phytoconstituents of *Enicostemma littorale* as potential glucokinase activators through molecular docking for the treatment of type 2 diabetes mellitus. *Silico Pharmacol* [Internet]. 2022;10(1). Available from: <https://doi.org/10.1007/s40203-021-00116-8>
30. Krzywinski M, Altman N. Points of significance: Significance, P values and t-tests. *Nat Methods*. 2013;10(11):1041–2.
31. Lipinski CA, Lombardo F, Dominy BW, Feeney PJ. Experimental and computational approaches to estimate solubility and permeability in drug discovery and development settings. Vol. 64, *Advanced Drug Delivery Reviews*. 2012. p. 4–17.